8-21-2014

Spin Dynamics and Magnetoelectric Properties of the Coupled-Spin Tetrahedral Compound Cu2Te2O5Cl2

Tiglet Besara

E. S. Choi

K.-Y. Choi

P. L. Kuhns

A. P. Reyes

See next page for additional authors

Recommended Citation

Besara, T., E. S. Choi, K-Y. Choi, P. L. Kuhns, A. P. Reyes, P. Lemmens, H. Berger, and N. S. Dalal. "Spin dynamics and magnetoelectric properties of the coupled-spin tetrahedral compound Cu 2 Te 2 O 5 Cl 2." Physical Review B 90, no. 5 (2014): 054418.

Spin dynamics and magnetoelectric properties of the coupled-spin tetrahedral compound $Cu_2Te_2O_5Cl_2$

T. Besara,[1,2] E. S. Choi,[2] K.-Y. Choi,[3,*] P. L. Kuhns,[2] A. P. Reyes,[2] P. Lemmens,[4,†] H. Berger,[5] and N. S. Dalal[1,2,‡]

[1]*Department of Chemistry and Biochemistry, Florida State University, Tallahassee, Florida 32306, USA*
[2]*National High Magnetic Field Laboratory, Florida State University, Tallahassee, Florida 32310, USA*
[3]*Department of Physics, Chung-Ang University, 84 Heukseok-ro, Seoul 156-756, Republic of Korea*
[4]*Institute for Condensed Matter Physics, TU Braunschweig, D-38106 Braunschweig, Germany*
[5]*Institute de Physique de la Matiere Complexe, EPFL, CH-1015 Lausanne, Switzerland*

(Received 22 September 2013; revised manuscript received 30 July 2014; published 21 August 2014)

We report on the spin dynamics and discovery of magnetoelectricity in the coupled-spin tetrahedral compound $Cu_2Te_2O_5Cl_2$. ^{125}Te NMR measurements show an anomalous resonance frequency shift and a signal wipe-out phenomenon around the Néel temperature $T_N = 18.2$ K, which could be attributed to the anomalous critical slowing down of the Cu spin fluctuations on the NMR time scale (∼10–100 MHz). The critical exponent of $(T_1T)^{-1} \propto (T - T_N)^{-\alpha}$ is 0.40 ± 0.03, as compared to 0.5 for a three-dimensional mean-field model. This is in contrast to the Br compound [S.-H. Baek *et al.*, Phys. Rev. B **86**, 180405 (2012)], which exhibits pronounced singlet dynamics with a large spin gap. Electric polarization (P_c) is observed along the c axis for temperatures below T_N under finite magnetic field but not sensitive to the electric poling. P_c increases sharply over zero to 2 T and then reaches saturation. Below T_N, P_c changes its sign depending on the applied magnetic field direction, positive for the $H \perp c$ axis and negative for $H \parallel c$ axis. We discuss possible explanations for the observed magnetoelectric (ME) behavior in terms of linear ME effect, spin-driven multiferroicity, and an exchange striction of intertetrahedral exchange paths involving the Te^{4+} lone-pair ions. Our results suggest that $Cu_2Te_2O_5Cl_2$ is a type of ME material whose properties are tuned by intertetrahedral exchange interactions involving polarizable Te^{4+} ions.

DOI: 10.1103/PhysRevB.90.054418 PACS number(s): 75.30.Kz, 76.60.−k, 77.80.B−

I. INTRODUCTION

Frustrated quantum spin systems have proven to be fertile ground for investigating novel quantum phenomena as well as multiferroicity. Examples of the former encompass spin liquids, spin-orbital quantum liquids, fractional spinon excitations, and magnetic monopoles [1]. The latter refers to magnetoelectric (ME) multiferroics, in which electric polarization is controllable by a magnetic field or magnetization is induced by an applied electric field [2]. This is due to the multifaceted role of competing magnetic interactions, i.e., frustration. On the one hand, it melts spin solids by enhancing quantum fluctuations, while on the other hand, it stabilizes incommensurate (ICM) magnetic structures with broken inversion symmetry, which compromises competing exchange interactions.

Experimentally, the aforementioned two aspects are seldom demonstrated in a single compound. The recently discovered $S = 1$ triangular antiferromagnet $Ba_3NiNb_2O_9$ is an exception, which exhibits concomitant up-up-down phase and multiferroicity [3]. The frustrated alternating spin-chain system $FeTe_2O_5Br$ shows both an ICM transverse amplitude modulated state and multiferroicity [4,5]. Particularly, the latter compound gives a hint for the search of ME materials accompanying frustration-induced novel magnetism. The key ingredient is the lone-pair cations (Te^{4+}, Se^{4+}, As^{3+}, and Sb^{3+}), which provide favorable conditions for the simultaneous occurrence of a frustrated spin topology and a high polarizability. This possibility has not yet been examined in the coupled-spin tetrahedral oxohalide $Cu_2Te_2O_5X_2$ ($X = Br, Cl$). For a decade, these compounds have attracted strong research interest from magnetism point of view [6–16]. However, not much is known about their dielectric/electric properties, and this provided the major impetus for the present study.

The basic magnetic unit of $Cu_2Te_2O_5X_2$ is a distorted tetrahedron made of four Cu^{2+} clusters [6–10]. The Cl compound shows an ICM antiferromagnetic ordering at $T_N = 18.2$ K [11]. The ordered magnetic moment of Cu^{2+} ions amounts to 0.88 μ_B, suggesting that the magnetic properties of the Cl compound may be rather approximated by a classical spin system in contrast to the Br compound. The field dependence of the ordering temperature determined by thermodynamic measurements follows a mean-field-like behavior [7]. Inelastic neutron-scattering studies revealed both Goldstone-like and gapped transverse modes. However, the size and intensity of the gapped excitations cannot be described within a mean-field or random-phase approximation theory [12,13]. Raman scattering measurements show coexistence of localized excitations and a broad two-magnon continuum, rare for conventional spin systems [14]. The inconsistency between the experiments and the conventional theories may signal either that no present theories are appropriate to describe coupled-spin tetrahedral systems or that magnetic excitations are mixed with a phonon mode due to ME interactions. In connection with the latter possibility, it is worth clarifying whether $Cu_2Te_2O_5Cl_2$ exhibits ferroelectricity.

In this paper, we present our systematic studies on $Cu_2Te_2O_5Cl_2$ single crystals by ^{125}Te NMR with the view of probing the critical properties of its spin excitations. In

*kchoi@cau.ac.kr
†p.lemmens@tu-bs.de
‡dalal@chem.fsu.edu

addition, we present data on the temperature and magnetic field dependence of its dielectric constant and electric polarization. The results clearly show that this compound is not a conventional ferroelectric, because its electric polarization is not reversible with the reversal of an applied electric field, unlike some related compounds in this class. On the other hand, it possesses unusual magnetoelectric properties that are controllable by applied magnetic fields whose underlying mechanism is not fully understood.

II. EXPERIMENTAL DETAILS

Single crystals of $Cu_2Te_2O_5Cl_2$ were prepared by the halogen vapor transport technique using $TeCl_4$ and Cl_2 as transport agents. Crystal quality has been confirmed to be high by extensive thermodynamic, magnetic, and spectroscopic measurements, excluding the presence of spurious phases [11,13,14]. ^{125}Te NMR spectra and relaxation times T_1 and T_2 of single crystals were obtained using a locally developed NMR spectrometer equipped with a high-homogeneity 14 T field-varying magnet. A typical dead time of the apparatus does not exceed 3 μs and a maximum pulse power is of 300–400 W. Our spectrometer is capable of pulses as short as 25 ns. The resonance spectra were obtained by sweeping the field at a fixed frequency. T_1 was measured by the standard $\pi/2 - \tau - \pi/2$ saturation recovery method, followed by a π pulse in order to create a Hahn echo. T_2 was measured by a $\pi/2 - \tau - \pi - \tau$ pulse sequence, resulting in a Hahn echo after the second delay time τ. Peak positions were determined by observing the highest point.

For dielectric measurements, contacts were made with silver paint on two flat surfaces of a single crystal in order to have parallel-plate capacitor geometry (typical dimension $2.5\times1.5\times0.4$ mm^3). Dielectric constant (ε') was obtained by measuring the capacitance of the sample using a General Radio capacitance bridge (frequency 1 kHz). The same sample was used for pyroelectric current measurement, where a transient current was recorded on warming after poling the crystal in an electric field while cooling down from above T_N. Spontaneous polarization (P) was obtained by integrating the pyroelectric current with respect to time.

III. RESULTS AND DISCUSSION

A. ^{125}Te NMR

^{125}Te ($I = 1/2$, $\gamma/2\pi = 13.454$ MHz/T) NMR measurements were performed on a single crystal of $Cu_2Te_2O_5Cl_2$ in the temperature range of 4–200 K. ^{125}Te was chosen over $^{63/65}$Cu, as the latter yielded a very complicated spectrum across a wide field range, while the former yielded relatively narrow lines. We thus focus on ^{125}Te NMR.

Figure 1 shows a unit cell of the crystal structure of $Cu_2Te_2O_5Cl_2$ projected onto the c axis (see Ref. [6] for more details on the crystal symmetry). Since the crystal symmetry contains four inequivalent Te sites, four peaks appear in an NMR spectrum when the crystal is aligned arbitrarily with respect to the applied field H [17]. In the field direction of $H//c$, however, the four sites become equivalent and thus the local symmetry of each Te atom is common along the c axis

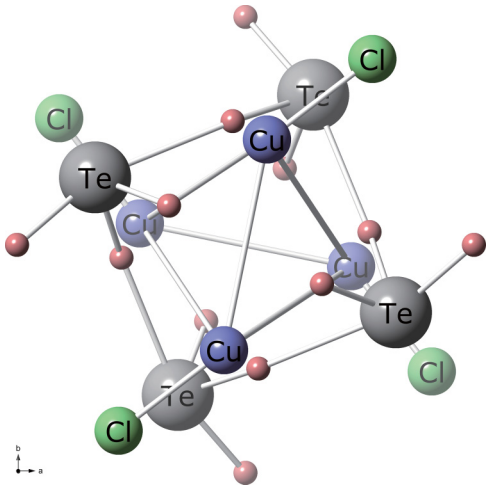

FIG. 1. (Color online) Crystal structure of $Cu_2Te_2O_5Cl_2$ along the c axis. The unlabeled atoms are the oxygen atoms.

(see in Fig. 1). As a result, the four lines collapse into a single peak.

Figure 2 shows the field-swept spectra obtained at a frequency of $\nu = 111$ MHz in the temperature range of $T = 20$–35 K, i.e., just above the phase transition T_N. The collapsing of the four lines into a single peak is illustrated in the upper inset of Fig. 2, where spectra of two different orientations (arbitrary and with applied field parallel to the c axis) are plotted against the Knight shift, a relative shift in the NMR frequency. In most of the measurements, the crystal was aligned with its c axis along the applied field in order to obtain a single peak. However, due to a slight misalignment, the peaks in the main panel of Fig. 2 show a slight broadening.

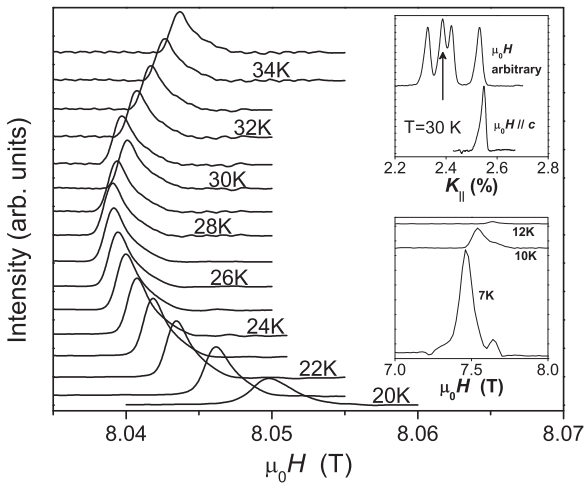

FIG. 2. Field-swept ^{125}Te NMR spectra of a single crystal of $Cu_2Te_2O_5Cl_2$ obtained by integrating spin-echo intensity as a function of temperature. The upper inset shows two field-swept spectra obtained at $T = 30$ K, one in an arbitrary field direction and one with $H||c$, plotted against the Knight shift. The arrow indicates the peak used for the relaxation measurements (see main text). The lower inset shows the spectra for temperatures below T_N, obtained at $\nu = 111$ MHz.

The bare nucleus at this resonance frequency would yield a signal at $H \approx 8.25$ T. As can be seen clearly in Fig. 2, all peaks in the temperature range shown are shifted at least by 0.2 T toward lower fields. Even at higher temperatures, shifts are clearly observed: a spectrum obtained at 200 K (not shown here) exhibits a shift of 0.08 T. This Knight shift is mainly due to the hyperfine coupling with the Cu electrons, but another contribution arises from the coupling with the Te electrons (i.e., chemical or orbital shift) [16–18]. The shift toward lower fields increases as the temperature decreases but reaches a maximum around 28 K, and subsequent spectra shift in the opposite direction, toward higher fields. This behavior reflects the spin susceptibility, which attains a maximum in essentially the same temperature regime, as can be seen in Fig. 4 (*vide infra*). The observed maxima in spectral shift and susceptibility are related to the short-range magnetic ordering, heralding the ensuing antiferromagnetic ordering at $T_N = 18.2$ K.

As the temperature is lowered further, the last obtainable spectrum is at 20 K before the signal completely disappears. This wipe-out effect is believed to be due to a significant reduction of the spin-spin relaxation time T_2 and/or a very large broadening of the spectrum, resulting from the magnetic transition, as was also reported for the sister compound $Cu_2Te_2O_5Br_2$ [17]. Unlike in Ref. [17], however, we regain the signal below the transition temperature at $T = 12$ K. Shown in the lower inset to Fig. 2 are the partial spectra below T_N, revealing the growing signal as the temperature is lowered further below T_N. Only the one peak in each spectrum that is closest to the zero shift position is displayed since each spectrum has many more peaks further away from the zero shift position (see Fig. 3). These spectra are much broader than those above T_N and are shifted significantly further. In this region, the ^{125}Te NMR spectrum becomes quite complicated due to the existence of ICM magnetic long-range ordering [11].

Figure 3 shows a wide-range field-swept spectrum taken at $T = 4.2$ K and $\nu = 111$ MHz. Evidence of ICM can be seen from the double-horn line shape of several of the peaks. Such a line shape is a signature of ICM ordering. Typically,

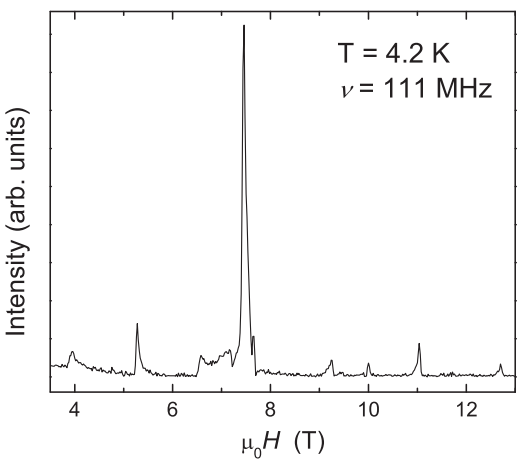

FIG. 3. Wide-range ^{125}Te NMR spectrum at $T = 4.2$ K, i.e., below the magnetic transition. The double-horn line shapes are a signature of incommensurate magnetic ordering.

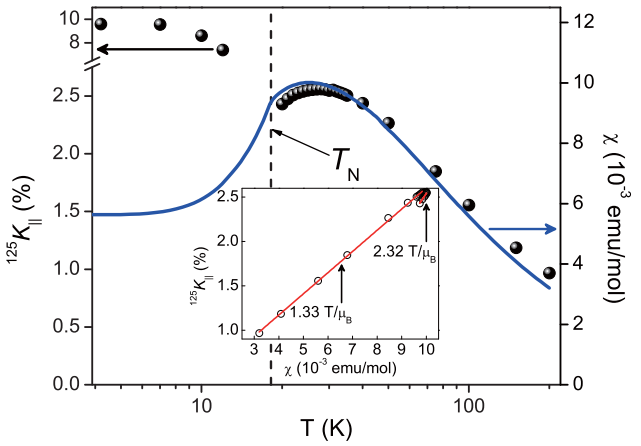

FIG. 4. (Color online) Temperature dependence of the magnetic shift K of the ^{125}Te nuclear spins measured in the field direction of $H//c$. The solid line is the SQUID (superconducting quantum interference device) susceptibility measurements. The inset shows a relative frequency shift of the NMR line versus dc susceptibility. The solid lines are the fits to Eq. (1).

however, the double-horn line shapes are closer to each other and with a clear continuum of intensities between the two peaks. Many pairs of the two peaks without a clear continuum feature indicate a complex spin structure due to slight structural distortions involved with magnetoelectricity (*vide infra*).

Figure 4 shows the temperature dependence of the magnetic shift and the susceptibility taken at a field of $H = 0.1$ T oriented along the c axis of the crystal. The susceptibility drops rapidly across the phase transition and then flattens out. The magnetic shift, on the other hand, experiences a different behavior: it increases to high values (7–10%), i.e., the peaks are shifted further toward lower fields, as can also be seen in the lower inset to Fig. 2. The discrepancy between the magnetic susceptibility and the magnetic shift for temperatures below T_N is due to the fact that the observed peak is one of the split peaks, a split arising from the ICM ordering. The other peak cannot be resolved due to an overlap with the extremely broad copper NMR spectra.

By correlating the magnetic shift with the susceptibility and taking the temperature as an implicit parameter, one can obtain information on the nuclear hyperfine field. In this so-called Clogston-Jaccarino plot [19] (i.e., Knight shift versus susceptibility), the slope of the line is a direct determination of the hyperfine field via

$$K_S(T) = K_{\text{chem}} + \frac{A_{hf}}{N_A \mu_B} \chi_{\text{spin}}(T). \qquad (1)$$

The first term is a (quite small) temperature-independent chemical or orbital shift, while the second term describes the shift due to hyperfine interactions. Here, A_{hf} represents the transferred magnetic hyperfine interaction between the Te nuclear spins and the Cu^{2+} electronic spins. The inset in Fig. 4 displays the Clogston-Jaccarino plot for the temperature region above the phase transition. In the high-temperature regime ($T = 30$–200 K), the hyperfine coupling constant is 1.33 ± 0.01 T/μ_B and increases to 2.32 ± 0.05 T/μ_B in the region directly above the phase transition ($T = 20$–25 K). Here we note that

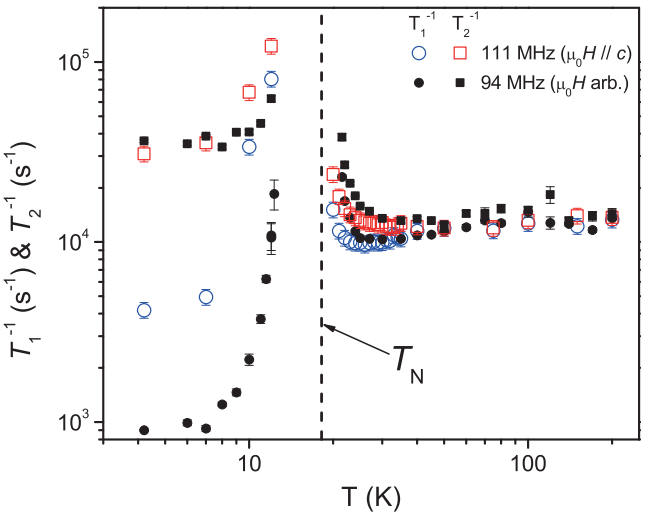

FIG. 5. (Color online) ^{125}Te spin-lattice relaxation rate $1/T_1$ (circles) and spin-spin relaxation rate $1/T_2$ (squares) on a logarithmic temperature scale at frequencies of $\nu = 111$ MHz (open symbols) and $\nu = 94$ MHz (filled symbols). The dashed vertical bar indicates the magnetic ordering temperature T_N.

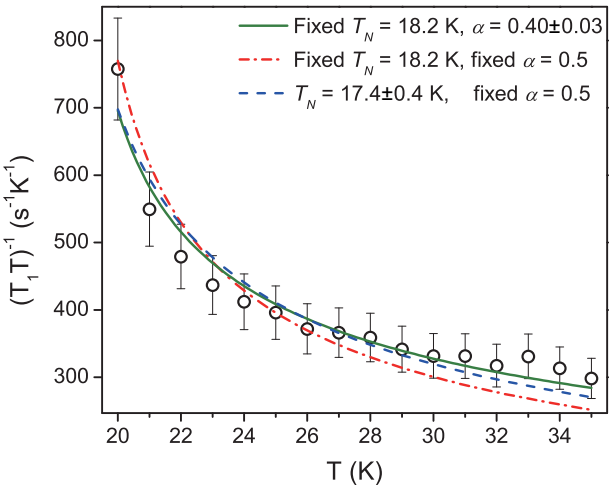

FIG. 6. (Color online) $(T_1T)^{-1}$ versus temperature at $\nu = 111$ MHz. The lines are fits to Eq. (2). See the text for details.

the obtained value of A_{hf} is rather large for a transferred hyperfine or direct dipolar fields from Cu^{2+} moments. Rather, this is typical of shifts due to ordered magnetic moments. This result shows that the hyperfine coupling constant contains contributions from short-range ordered Cu^{2+} spins. Thus the increase of A_{hf} with decreasing temperature can be interpreted in terms of a dimensional crossover of magnetic correlations. At $T > 30$ K, magnetic correlations are governed by intratetrahedral interactions. As the temperature is lowered from 25 K toward T_N, they become of a three-dimensional nature due to intertetrahedral interactions.

To study spin dynamics, we also performed relaxation measurements across the magnetic phase transition. Figure 5 displays the temperature dependence of two sets of spin-lattice relaxation rate (T_1^{-1}) and spin-spin relaxation rate (T_2^{-1}) measurements: one obtained at $\nu = 111$ MHz with the crystal aligned in the field direction of $H//c$ (open symbols), and the other at $\nu = 94$ MHz with the crystal aligned arbitrarily (filled symbols). The latter set yielded four peaks, and the relaxation measurements were performed on the second-to-lowest peak of the four (see the arrow in the upper inset to Fig. 2). The two sets do not deviate much from each other in the paramagnetic region, and both relaxation rates decrease steadily as the temperature is lowered. However, around 35 K and until the signal vanishes, both T_1^{-1} and T_2^{-1} increase rapidly. As mentioned earlier, the divergence may be a reason for the vanishing of the signal, below $T = 20$ K for the 111 MHz and below $T = 21.5$ K for the 94 MHz case; the relaxation times simply become too short to be measured. In both cases, the signal reappears below the transition temperature at $T = 12$ K, and the rates decrease as the temperature is lowered. The spin-lattice relaxation rates decrease rapidly (over an order of magnitude) and give a hint of flattening out at the lowest temperatures, while the spin-spin relaxation rates decrease less dramatically and flatten out earlier, at around $T = 8$ K.

The anomalous increase of T_1^{-1} and T_2^{-1} with decreasing temperature is a sign of critical slowing down of the Cu spin fluctuations [20], evidence of a phase transition to a long-range magnetic ordering (see Fig. 5). The sharpness of the spin-lattice relaxation rates indicates that the ordering is of three-dimensional antiferromagnetic nature. To investigate this, we fit the divergence to the following relation:

$$\frac{1}{T_1 T} \propto (T - T_N)^{-\alpha}, \tag{2}$$

where α is the critical exponent and T_N is the Néel temperature. A critical exponent of $\alpha = 0.5$ would indicate three-dimensional fluctuations of local antiferromagnetic moments [21]. Figure 6 shows a plot of $(T_1T)^{-1}$ as a function of temperature for the case of $\nu = 111$ MHz in the vicinity of the phase transition, along with different fits to the relation in Eq. (2). By fixing the transition temperature to $T_N = 18.2$ K and using Eq. (2) to fit the data, we obtain the critical exponent $\alpha \approx 0.40 \pm 0.03$ (green solid line in Fig. 6), which is in fairly good agreement with the 3D AFM picture mentioned above. By also fixing the exponent to $\alpha = 0.5$, it is clear that the fit agrees less well with the data (red dashed-dotted line in Fig. 6). One issue that should be considered is the wipe-out effect, which does not allow fitting of data down to T_N, and therefore affects the curve. By relaxing T_N, while keeping the exponent fixed at $\alpha = 0.5$, we obtain a Néel temperature of $T_N \approx 17.4 \pm 0.4$ K (blue dashed line in Fig. 6), which clearly is inside the wipe-out region. It is worth noting that by relaxing both T_N and α we obtain a Néel temperature very close to 20 K, clearly being affected by the fact that the last obtainable spectrum is at 20 K. It is obvious that the wipe-out effect hinders us from obtaining a reasonable fitting of the $(T_1T)^{-1}$ data; however, we can say that the data most likely does support the picture of a three-dimensional antiferromagnetic ordering.

We now compare our results to those for the Br compound $Cu_2Te_2O_5Br_2$, which lies in proximity to a quantum critical point, i.e., it shows enhanced quantum fluctuations. This is reflected in a strongly reduced ordered moment of 0.4 μ_B and reduced transition temperature of $T_N = 11.4$ K [22].

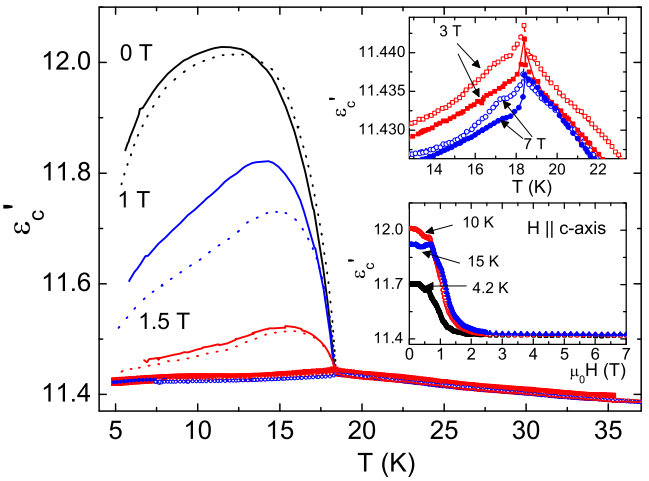

FIG. 7. (Color online) Temperature dependence of dielectric constant (ε_c') with the electric field parallel to the c axis. The magnetic field is applied either parallel (solid line or solid symbol) or perpendicular (dotted line or open symbol) to the c axis. Upper inset: expansion of ε_c' around the transition. Lower inset: magnetic field dependence of ε_c' for $H//c$.

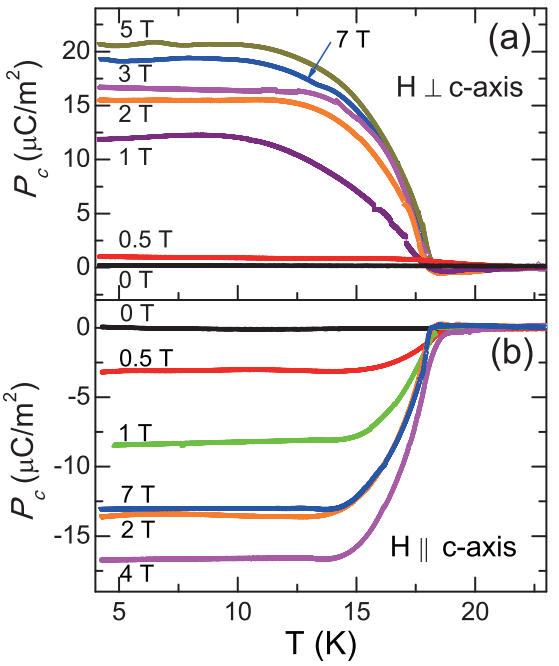

FIG. 8. (Color online) Temperature dependence of electric polarization (a) for $H \perp c$ and (b) $H//c$.

In the paramagnetic state, $1/T_1$ of the Br compound shows a thermally activated behavior with a spin gap of ∼56 K [16]. This suggests that singlet fluctuations govern the spin dynamics. In contrast, for the Cl compound we observe a much-reduced spin gap of 7.4 K (not shown here). The NMR results are consistent with inelastic neutron and light-scattering measurements [13,14], which show dispersive and flat magnetic excitations. For the Cl compound, the low-temperature excitation spectrum is dominated by the dispersive band, which strongly broadens and softens at elevated temperatures. In the Br compound, however, most of the spectral weight remains gapped for temperatures well above T_N. This contrasting behavior of the Br and Cl compound may be associated with their difference in the strength and frustration of intertetrahedral interactions [15].

B. Dielectric constant and electric polarization

Figure 7 shows the temperature dependence of the dielectric constant along the c axis (ε_c') with different applied magnetic fields. The electric field is applied parallel to the c axis. At zero magnetic field, ε_c' increases abruptly at T_N, followed by a broad maximum at around $T = 13$ K upon further cooling. A steplike anomaly is not compatible with a ferroelectric material but it is typical for a usual magnetic material. With increased magnetic fields, the rapid increase of ε_c' just below T_N becomes less significant and almost field independent for $H > 2.5$ T. A closer examination of ε_c' for $H = 3$ and 7 T (see the upper inset of Fig. 7) revealed a λ-shaped anomaly at T_N. This is in stark contrast to the steplike anomaly observed at zero field and reminds us of a paraelectric-to-ferroelectric transition or paramagnetic-AFM transition with linear ME effect [23,24]. For samples with electric fields perpendicular to the c axis, the anomaly around T_N is very small, possibly due to a misalignment of the sample, and shows no field dependence (data not shown).

To investigate the origin of the dielectric constant anomaly, we measured the electric polarization (P) of $Cu_2Te_2O_5Cl_2$ around T_N. To obtain the polarization, a pyroelectric current (I_p) was measured while warming up after the sample was cooled down under both magnetic and electric field (ME cooling) to ensure a single ME domain. All the data were taken in the presence of corresponding magnetic field, while the electric poling dependence was checked for $H_{\perp c} = 7$ T. Interestingly, I_p was found insensitive to the electric poling, as the I_p curves taken under different poling electric fields are practically identical [see Fig. 9(a)]. All the other data shown in Fig. 8 were taken under the constant poling electric field of +190 kV/m for consistency.

Figure 8 shows the temperature dependence of the polarization along the c axis (P_c) for two different magnetic field directions, parallel or perpendicular to the c axis. At zero magnetic field, P_c is almost zero, even though the dielectric constant shows distinctive anomalies at T_N. On applying a magnetic field, P_c increases sharply at low fields below 2 T and starts to saturate at higher fields. Interestingly, this magnetic field dependence of P_c is similar to that of ε_c' (see the lower inset of Fig. 7). It is noted that the value of the saturation electric polarization is about 20–30 times smaller than those of orthorhombic perovskite rare-earth manganites but it is comparable to that of $FeTe_2O_5Br$ [5,25]. Another distinct feature is the change of sign of P_c depending on the applied magnetic field direction—positive for the $H \perp c$ axis and negative for the $H \parallel c$ axis.

There are at least four notable features of the ME behavior of $Cu_2Te_2O_5Cl_2$: (1) dielectric constant anomalies below T_N, the large sharp steplike increase at zero field and λ-shaped anomaly under magnetic field; (2) field-induced polarization and its saturation behavior at higher fields above 2 T; (3) polarization sign change under different field directions; and

(4) electric polarization not reversible with the change in the sign of the poling electric field.

The absence of the electric polarization reversibility on reversing the electric field direction [feature (4)] is quite unusual for ferroelectric or ME materials, where poling is required to achieve a single ME domain. We note, however, that recently, similar polarization irreversibility was observed in the multiferroic $Ba_3NbFe_3SiO_{14}$ [26], which was attributed to a self-formed single ME domain. $Ba_3NbFe_3SiO_{14}$ is known to form a single magnetic domain in the ordered state, which is a prerequisite condition to form the single ME domain. For $Cu_2Te_2O_5Cl_2$, it was found that a moderate field of 2 T produced a monodomain (single magnetic domain) ground state [13], from which we may conjecture that the single ME domain is also formed in $Cu_2Te_2O_5Cl_2$ for $H < 7$ T.

The other observed ME behaviors [features (1)∼(3)] are not well explained with current understanding of the spin-driven ferroelectricity or ME effect. First of all, the emergence of P_c only under finite magnetic fields cannot be accounted for by the models developed for spiral magnets [27,28]. According to the models, for the reported magnetic structure of $Cu_2Te_2O_5Cl_2$ [22], one can predict finite P_c even at zero magnetic field, which will gradually decrease as the external field rotates the spiral planes. The feature (2) obviously contradicts to the prediction.

The quasilinear increase of P_c with field is more reminiscent of the linear ME effect, which occurs when both space inversion and time-reversal symmetries are broken as in $Cu_2Te_2O_5Cl_2$. For the linear ME effect, polarization along the i axis (P_i) can be expressed as $P_i = \alpha_{ij} H_j$, where α_{ij} is the linear ME tensor and H_j is the external magnetic field. In our work, we found $P_a \approx P_b \approx 0$ and P_c ($=\alpha_{ca} H_a + \alpha_{cb} H_b + \alpha_{cc} H_c$) > 0 for $H_c = 0$ and $P_c < 0$ for $H_c \neq 0$. To be more specific, the linear coefficient $\alpha_{cc} \sim -2\times10^{-4}$ CGS unit and $\alpha_{\parallel}\sim3\times10^{-4}$ CGS unit are extracted from the slope of $|P_c|$ versus H. [See the dashed lines in Fig. 9(b).] There are different forms of linear ME tensors for different magnetic point groups [29], but none of them is applicable to our experimental results. Moreover, the linear ME effect predicts no dielectric constant anomaly at zero magnetic field, which is not the case in $Cu_2Te_2O_5Cl_2$.

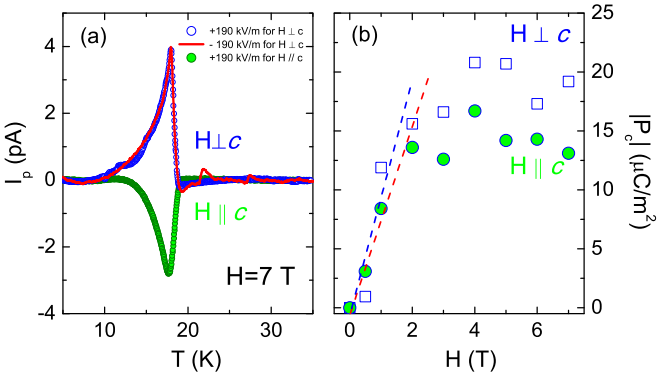

FIG. 9. (Color online) (a) Pyroelectric current at $H = 7$ T for different poling electric fields of +190 (blue open circles) and −190 kV/m (red solid line) for H⊥c and +190 kV/m (full green circles) for H//c configuration. The curves for $H \perp c$ are lying on top of each other. (b) Magnetic field dependence of the absolute value of polarization ($|P_c|$) measured at $T = 5$ K. The dashed lines are linear fits to $|P_c|$ for fields below 2 T.

Here we recall that in the tellurite-oxohalide $FeTe_2O_5Br$, the direction of P predicted by the above models is different from that experimentally observed [4]. In that case, a microscopic origin of the ME effect was attributed to the exchange striction of the intercluster super-superexchange interaction Fe-O-Te-O-Fe [5]. The low-symmetry exchange pathway involving polarizable Te^{4+} lone-pair ions concomitantly induces frustration and thus the ICM magnetic ordering as well as the electric polarization. This allows for the establishment of a sizable ME coupling with small changes in the strength of the exchange interaction because easily polarizable Te^{4+} ions mediate long exchange paths. The same exchange striction mechanism may be applied to $Cu_2Te_2O_5Cl_2$, where intertetrahedral couplings are partly mediated by Te^{4+} ions. We also note that exchange striction does not generally require an external magnetic field to induce polarization, which is true in the case of $FeTe_2O_5Br$ but not in $Cu_2Te_2O_5Cl_2$. To explain this discrepancy, one may conjecture a combined effect of the ME and magnetostriction [30]. In this mechanism, local deviation of the ordered magnetization can arise from magnetostriction in the grains and their boundaries, which in turn generates local electric fields (induces polarization) through the ME effect. In the vicinity of the transition, the locally deviated moment increases with external magnetic field, leading to increased polarization. In addition, the polarization anisotropy under magnetic field can be readily understood by the different ME coefficients along the different field directions.

Our results suggest that the tellurite-oxohalide compounds are susceptible to ME effects due to the long exchange bridges hosting Te^{4+} lone-pair ions. Density functional theory calculations [5,10] reveal that the super-superexchange interactions by lone-pair ions in the oxohalides are non-negligible. Rather, these interactions are often the key to understanding magnetic and electric properties as well as the ME coupling. Noticeably, Prša *et al.* [13] attribute the coexistence of a weak Goldstone-like mode and the size of the energy gaps to intercluster quantum fluctuations. In multiferroic materials, low-energy excitations are electromagnons, which are hybrid spin and lattice excitations. One cannot ignore that the low-energy spin excitations observed in $Cu_2Te_2O_5X_2$ may be coupled to lattice excitations. In this case, a spin model alone may be insufficient to give a full account of the anomalous low-lying excitations. Based on our results, we propose to examine the effects of ME coupling on elementary excitations.

IV. CONCLUSIONS

We have presented detailed ^{125}Te NMR and dielectric measurements on the coupled-spin tetrahedral compound $Cu_2Te_2O_5Cl_2$. We observe a strong effect of applied magnetic field on dielectric constant and electric polarization: the sign of the electric polarization is opposite for the magnetic field applied along or perpendicular to the crystal symmetry axis, so also above or below T_N. We also observed insensitivity of the polarization to the electric poling, which may indicate a self-formed single ME domain. The observed ME behavior is still not well understood by *current* models of spin-driven

ferroelectricity or ME effect, which has been left as an open question. More studies are needed, including ME cooling dependence at different magnetic fields and polarization under different configurations to elucidate the underlying mechanism of the ME behavior.

As to spin dynamics, an earlier ^{125}Te NMR study of the Br compound showed pronounced singlet fluctuations with a large spin gap of 56 K [16]. The present ^{125}Te NMR resonance frequencies as well as the relaxation times T_1 and T_2 exhibit a signal wipe-out effect related to the anomalous shortening of T_2 and a large reduction of a spin gap to 7.4 K. This suggests a substantial softening of gapped spectral weights due to stronger intertetrahedral couplings.

Our work demonstrates that in tellurite oxohalides, intertetrahedral exchange interactions are important in understanding magnetic and magnetoelectric properties. The applicability of this finding should be examined in other oxohalide compounds hosting lone-pair cations (Te^{4+}, Se^{4+}, As^{3+}, and Sb^{3+}). While further studies are needed to explain some of these observations, it is clear that these materials are a forerunner of an interesting class of magnetoelectric materials.

ACKNOWLEDGMENTS

The National High Magnetic Field Laboratory is supported by the NSF Cooperative Agreement No. DMR-1157490, the State of Florida and the U.S. Department of Energy. We thank acknowledge financial support from the Korea NRF (Grant No. 2012-046138), German-Israeli Foundation (GIF, 1171-486 189.14/2011), the NTH-School "Contacts in Nanosystems: Interactions, Control and Quantum Dynamics", the Braunschweig International Graduate School of Metrology, and DFG-RTG 1953/1, Metrology for Complex Nanosystems. We thank K. Schnettler for important help and an anonymous referee for an important remark on the relevance of the ME behavior in $Cu_2Te_2O_5Cl_2$.

[1] L. Balents, Nature (London) **464**, 199 (2010).
[2] S. W. Cheong and M. Mostovoy, Nat. Mater. **6**, 13 (2007).
[3] J. Hwang, E. S. Choi, F. Ye, C. R. Dela Cruz, Y. Xin, H. D. Zhou, and P. Schlottmann, Phys. Rev. Lett. **109**, 257205 (2012).
[4] M. Pregelj, O. Zaharko, A. Zorko, Z. Kutnjak, P. Jeglic, P. J. Brown, M. Jagodic, Z. Jaglicic, H. Berger, and D. Arcon, Phys. Rev. Lett. **103**, 147202 (2009).
[5] M. Pregelj, H. O. Jeschke, H. Feldner, R. Valenti, A. Honecker, T. Saha-Dasgupta, H. Das, S. Yoshii, T. Morioka, H. Nojiri, H. Berger, A. Zorko, O. Zaharko, and D. Arcon, Phys. Rev. B **86**, 054402 (2012).
[6] M. Johnsson, K. W. Tornroos, F. Mila, and P. Millet, Chem. Mater. **12**, 2853 (2000).
[7] P. Lemmens, K.-Y. Choi, E. E. Kaul, C. Geibel, K. Becker, W. Brenig, R. Valentí, C. Gros, M. Johnsson, P. Millet, and F. Mila, Phys. Rev. Lett. **87**, 227201 (2001).
[8] P. Lemmens, K.-Y. Choi, A. Ionescu, J. Pommer, G. Güntherodt, R. Valentí, C. Gros, W. Brenig, M. Johnsson, P. Millet, and F. Mila, J. Phys. Chem. Solids **63**, 1115 (2002).
[9] P. Lemmens, K.-Y. Choi, G. Güntherodt, M. Johnsson, P. Millet, C. Gros, and W. Brenig, Physica B **329-333**, 1049 (2003).
[10] R. Valentí, T. Saha-Dasgupta, C. Gros, and H. Rosner, Phys. Rev. B **67**, 245110 (2003).
[11] O. Zaharko, A. Daoud-Aladine, S. Streule, J. Mesot, P.-J. Brown, and H. Berger, Phys. Rev. Lett. **93**, 217206 (2004).
[12] S. J. Crowe, S. Majumdar, M. R. Lees, D. McK. Paul, R. I. Bewley, S. J. Levett, and C. Ritter, Phys. Rev. B **71**, 224430 (2005).
[13] K. Prša, H. M. Rønnow, O. Zaharko, N. B. Christensen, J. Jensen, J. Chang, S. Streule, M. Jiménez-Ruiz, H. Berger, M. Prester, and J. Mesot, Phys. Rev. Lett. **102**, 177202 (2009).
[14] K.-Y. Choi, H. Nojiri, N. S. Dalal, H. Berger, W. Brenig, and P. Lemmens, Phys. Rev. B **79**, 024416 (2009).
[15] X. Wang, K. Syassen, M. Johnsson, R. Moessner, K.-Y. Choi, and P. Lemmens, Phys. Rev. B **83**, 134403 (2011).
[16] S.-H. Baek, K.-Y. Choi, H. Berger, B. Büchner, and H.-J. Grafe, Phys. Rev. B **86**, 180405 (2012).
[17] A. Comment, H. Mayaffre, V. Mitrović, M. Horvatić, C. Berthier, B. Grenier, and P. Millet, Phys. Rev B **82**, 214416 (2010).
[18] I. Orion, J. Rocha, S. Jobic, V. Abadie, R. Brec, C. Fernandez, and J.-P. Amoureux, J. Chem. Soc. Dalton Trans. 3741 (1997).
[19] A. M. Clogston and V. Jaccarino, Phys. Rev. **121**, 1357 (1961).
[20] T. Moriya, J. Phys. Soc. Jpn. **18**, 516 (1963).
[21] T. Moriya and K. Ueda, Solid State Commun. **15**, 169 (1974).
[22] O. Zaharko, H. Rønnow, J. Mesot, S. J. Crowe, D. M. Paul, P. J. Brown, A. Daoud-Aladine, A. Meents, A. Wagner, M. Prester, and H. Berger, Phys. Rev. B **73**, 064422 (2006).
[23] N. Mufti, G. R. Blake, M. Mostovoy, S. Riyadi, A. A. Nugroho, and T. T. M. Palstra, Phys. Rev. B **83**, 104416 (2011).
[24] A. Iyama and T. Kimura, Phys. Rev. B **87**, 180408(R) (2013).
[25] T. Kimura, G. Lawes, T. Goto, Y. Tokura, and A. P. Ramirez, Phys. Rev. B **71**, 224425 (2005).
[26] N. Lee, Y. J. Choi, and S.-W. Cheong, Appl. Phys. Lett. **104**, 072904 (2014).
[27] H. Katsura, N. Nagaosa, and A. V. Balatsky, Phys. Rev. Lett. **95**, 057205 (2005).
[28] I. A. Sergienko and E. Dagotto, Phys. Rev. B **73**, 094434 (2006).
[29] H. Schmid, J. Phys.: Condens. Matter **20**, 434201 (2008).
[30] J. Hwang, E. S. Choi, H. D. Zhou, J. Lu, and P. Schlottmann, Phys. Rev. B **85**, 024415 (2012).